

# Global two-monopoles

Sven Bjarke Gudnason<sup>\*</sup> and Jarah Evslin<sup>†</sup>

Institute of Modern Physics, Chinese Academy of Sciences, Lanzhou 730000, China

## Abstract

Global two-monopoles are unstable in their simplest formulation. We construct a model with a metric-like prefactor which we show can stabilize the global two-monopoles. The stabilizing construction is realized with a Skyrme sector where the metric-like prefactor is a function of the Skyrmon profile.

November 13, 2015

---

<sup>\*</sup>bjarke(at)impcas.ac.cn

<sup>†</sup>jarah(at)impcas.ac.cn

# 1 Introduction

If the set of minima  $\mathcal{M}$  of the potential energy of a field is not 2-connected, for example if it is a 2-sphere  $S^2$  or real projective space  $\mathbb{RP}^2$ , then it admits solutions called global monopoles. In general the total energy of a global monopole exhibits a long distance divergence (linear divergence).

In the literature the global monopole has been considered mostly in a cosmological context where the gravitational energy, their Goldstone boson radiation and gravitational-wave emission and finally pair annihilation sparked the primary interest [1, 2, 3]. Global monopoles may also be realized in nematic fluids [4].

The stability of a single global monopole has been debated in the early literature. It was argued that the global monopole could itself collapse to a zero-energy solution [5], but it was shortly after argued not to hold true [6]. Ref. [7] further argued that the observation of Ref. [5] should not be interpreted as a collapse but rather as an acceleration of the entire monopole. The false conclusion was thus reached by artificially holding the origin of the monopole fixed. The bottom line is that the single global monopole is indeed stable, both with respect to radial and angular perturbations [7].

Ref. [7] made a further study of the mutual forces between two different types of a global monopole and an anti-monopole, which we will call type B and type C. We find – in agreement with Ref. [7] – that the type C monopole and anti-monopole attract each other and the type B repel each other. We find, however, different values of the forces than Ref. [7] does. We further generalize this calculation to two monopole-monopole cases which we will call type A and type B and they are both mutually repulsive.

The literature has nothing much to report about global multimonopole configurations. This is because they are unstable. For completeness we carry out a numerical calculation of a perturbed two-monopole configuration in Appendix A to confirm that they are indeed unstable; that is they repel.

We contemplate an interaction term which may be added to the global monopole Lagrangian in order to stabilize said system. This is argued, however, to be problematic due to the possibility that the monopoles just to shrink upon such an intervention. We have also checked this with numerical calculations.

As a different approach on the path to stabilize the global two-monopole configura-

tion, we consider a modification of the global monopole Lagrangian more similar to a nontrivial effective metric. We choose to construct said effective metric being a function of a Skyrme field. The stabilization is thus dynamic but not renormalizable. The Skyrme Lagrangian [8, 9] itself is not renormalizable either, so we do not regard that as a big problem but the model as an effective field theory model generated by some fundamental theory. A single gauged monopole inside a U(1) gauged single Skyrme has been studied in the literature already [10]. We are studying the global analog of such a configuration and the multimonomopole instead of the single monopole. We show that the global two-monopole can indeed be stabilized inside a Skyrme for certain choices of parameters.

The paper is organized as follows. In the next section we review a single global monopole to remind the reader and set the notation. In Sec. 3 we review the monopole-anti-monopoles interactions in the point-charge approximation and make the same type of analysis for the two-monopole system. After Sec. 3 we no longer use the point-charge approximation and all the calculations and considerations are carried out with the monopole profile functions and hence with true equations of motion. In Sec. 4 we discuss the possibility of stabilizing the global two-monopole using an interaction term. In Sec. 5 we construct the two-monopole inside a Skyrme and dub it the Skyrmonopole. Finally, we conclude in Sec. 6. The Appendix A presents a numerical calculation showing the instability of the normal global two-monopole.

## 2 A single global monopole

The theory consists of an adjoint-valued scalar field,  $\Phi = \Phi^a \sigma^a$ , the gauge indices  $a = 1, 2, 3$  are summed over,  $\sigma^a$  are the Pauli matrices and the Lagrangian density is

$$\mathcal{L} = -\frac{v^2}{2} \text{Tr}(\partial_\mu \Phi)^2 - \frac{\lambda v^4}{4} (1 - \text{Tr}[\Phi^2])^2, \quad (2.1)$$

which has the equation of motion

$$\partial_\mu \partial^\mu \Phi = -\lambda v^2 (1 - \text{Tr}[\Phi^2]) \Phi. \quad (2.2)$$

The Greek letters are used for spacetime indices,  $\mu = 0, 1, 2, 3$  and we use the mostly-positive metric. The potential breaks the global SO(3)-symmetry down to SO(2) and the coset SO(3)/SO(2)  $\sim S^2$  when mapped from spatial infinity, which is also  $S^2$ , defines the topological charge by means of the second homotopy group. The topological charge of the monopole is given by the winding number, i.e.

$$Q = -\frac{1}{8\pi} \oint dS^{ij} \epsilon_{abc} \Phi^a \partial_i \Phi^b \partial_j \Phi^c, \quad (2.3)$$

where  $a, b, c = 1, 2, 3$  are gauge indices and  $i, j = 1, 2, 3$  are spatial indices. The charge  $Q$  is also called the monopole number. The mass of the monopole is the total energy in the rest frame

$$E[\Phi] = - \int d^3x \mathcal{L}[\Phi]. \quad (2.4)$$

Let us first review the standard hedgehog configuration which describes a single global monopole in the theory at hand. Since  $Q = 1$ , we can use a spherical Ansatz

$$\Phi = \frac{1}{r} h(r) x^a \sigma^a, \quad (2.5)$$

for which the energy density reads

$$\frac{1}{v^2} \mathcal{E} = \frac{1}{2} (h')^2 + \frac{1}{r^2} h^2 + \frac{\lambda v^2}{4} (h^2 - 1)^2, \quad (2.6)$$

where  $' = \partial_r$ . Defining a dimensionless coordinate,  $\rho \equiv \sqrt{\lambda} v r$ , we can write the energy density as

$$\frac{1}{\lambda v^4} \mathcal{E} = \frac{1}{2} (h')^2 + \frac{1}{\rho^2} h^2 + \frac{1}{4} (h^2 - 1)^2, \quad (2.7)$$

where  $h = h(\rho)$ ; now  $' = \partial_\rho$  and the equation of motion reads

$$h'' + \frac{2}{\rho} h' - \frac{2}{\rho^2} h - (h^2 - 1)h = 0. \quad (2.8)$$

The boundary conditions for the monopole are:  $h(0) = 0$  and  $h(\infty) = 1$ . Expanding around  $\rho = 0$ , we get

$$h = a\rho - \frac{a}{10}\rho^3 + \frac{a + 10a^3}{280}\rho^5 + \mathcal{O}(\rho^7), \quad (2.9)$$

where  $a > 0$  is a constant (also called the shooting parameter). This tells us that the energy density around the center goes as

$$\frac{1}{\lambda v^4} \mathcal{E} = \left( \frac{1}{4} + \frac{3}{2}a^2 \right) - a^2 \rho^2 + \left( \frac{9}{50}a^2 + \frac{1}{2}a^4 \right) \rho^4 + \mathcal{O}(\rho^6), \quad (2.10)$$

i.e. roughly constant for small values of  $a$ . Asymptotically,  $h$  is very close to one, so linearizing about  $\beta = 1 - h$ , we get the asymptotic equation of motion

$$\beta'' + \frac{2}{\rho} \beta' - \frac{2}{\rho^2} (\beta - 1) - 2\beta = 0, \quad (2.11)$$

which has the exact solution

$$h = 1 - \beta = 1 - \frac{1}{\rho^2}. \quad (2.12)$$

This in turn determines the asymptotic energy density as

$$\frac{1}{\lambda v^4} \mathcal{E} = \frac{1}{\rho^2} - \frac{1}{\rho^4} + \frac{2}{\rho^6} + \frac{1}{4\rho^8}, \quad (2.13)$$

which for large  $\rho$  goes like  $1/\rho^2$  and hence the total energy diverges linearly. Finally, the topological charge can easily be calculated using Eq. (2.3) as

$$Q = -\frac{1}{8\pi} \oint dS^{ij} \epsilon_{aij} h^3 \frac{x^a}{r^3} = 1. \quad (2.14)$$

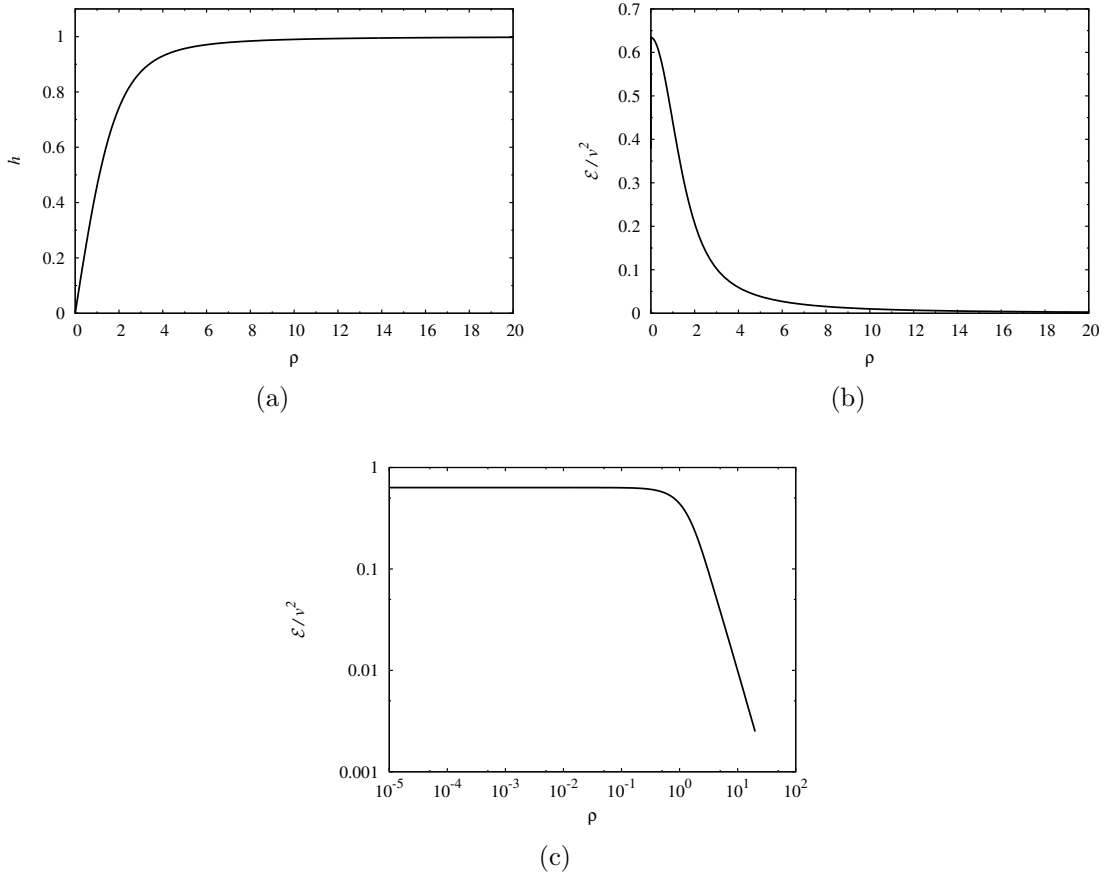


Figure 1: (a) profile function  $h$ , (b) energy density and (c) energy density on loglog scale for the hedgehog ( $Q = 1$ ) monopole.

In Fig. 1 is shown the profile function and energy density of the hedgehog configuration.

### 3 Charge-two and charge-zero monopoles in the point-charge approximation

Let us now turn to the double-winding global monopole configuration. The overall orientation of the monopole is not important, but the relative orientation is important for the multi-monopole solution. In the following we will write the scalar field as

$$\Phi = h \{ \sin g \cos k, \sin g \sin k, \cos g \}, \quad (3.1)$$

which describes a charge-two monopole if  $k$  winds twice and  $g$  winds once. Another possibility is to make  $g$  wind two times and  $k$  one time, but it requires a twist (sign change) of for instance  $k$ , in order not to create a monopole-anti-monopole pair. To see the charge explicitly, let us evaluate the integral (2.3) for  $g = m\theta$  and  $k = n\phi$  at some asymptotic distance where  $h = 1$ :

$$Q = \frac{1}{8\pi} \oint dS^{ij} \epsilon_{abc} \Phi^a \partial_i \Phi^b \partial_j \Phi^c = n \sin^2 \left( \frac{m\pi}{2} \right). \quad (3.2)$$

We will study a number of cases in turn.

For physical and everywhere regular global monopoles, the profile function  $h$  cannot take the value 1 over all space, but should have at least  $Q$  zeros, counted with multiplicity. Regularity dictates that the zeros of  $h$  coincide with the origins of where the phases of  $g$  and  $k$  wind about. The approximation of setting  $h := 1$  can physically be seen as the limit of very small monopole sizes compared to the separation distances. Once we set  $h := 1$ , we introduce singularities at these origins or positions of the charges. These singularities are dealt with by subtracting the same singularity of a single singular global monopole field. The difference is then a regular field. This approximation captures the asymptotic interaction of global monopoles, where the potential has no effect, but only the winding phases interact at long distances via the kinetic term. This interaction is important as it can never be neglected.

Independent of the local regularity of the global monopole, the total energy of the configuration always diverges linearly. This divergence is just an artifact of putting a global monopole in an infinite space. In real world applications, such as liquid crystals, global monopoles only live in a finite region of space. In this paper we will consider the global monopoles on an infinite space, although the numerical calculations will of course only be carried out on a finite space, just like the physical global monopoles enjoy.

A comment is in order about the Ansätze that we will use for the function  $g$  and  $k$  in the next subsections. They are not describing *solutions*, but describe the winding

that necessarily will be present on a given timeslice in a would-be solution. Logically, there are two possible situations. If the two charges attract, a solution will be close to a configuration where the charges are coincident. By making an educated guess for the function  $h$ , the full, time-dependent solution can then be found using the full equations of motion. The other possibility is that the charges repel each other. In that case, no stable solution exists and this type of configuration is never a static solution, but at best a snapshot of a time dependent field configuration that evolves in time. Real time dependent solutions to the equations of motion can be constructed, but since we are not interested in unstable time dependent configurations, we will simply disregard such cases as being what they are: unstable.

### 3.1 Type A

The first case is the charge-two monopole where  $k$  winds twice and  $g$  once

$$\Phi_{\text{full}} = h \{ \sin \theta \cos(\phi_1 \pm \phi_2), \sin \theta \sin(\phi_1 \pm \phi_2), \cos \theta \}, \quad (3.3)$$

where we define the angles as

$$\theta = \arccos \frac{z}{r}, \quad \phi_1 = \arctan \frac{y}{x-d}, \quad \phi_2 = \arctan \frac{y}{x+d}, \quad (3.4)$$

and the two monopole charges are separated by a distance  $2d$ . We will treat a case of a monopole-anti-monopole on the same footing as the monopole-monopole by choosing the lower sign. The monopole charge of the configuration does not depend on  $d$ ; hence if we set  $d = 0$ , we can see from Eq. (3.2) that this configuration has charge 2 for the upper sign and charge zero for the lower sign.

In order to study the stability of this monopole, let us make a point-charge approximation, where  $h := 1$ . This approximation corresponds to ignoring the potential and taking into consideration the asymptotic effect of two charges affected only by the kinetic term. See also the discussion in the previous subsection.

The form (3.3) has been chosen for its simplicity. However the price of this simple form is that, when  $d \neq 0$ , the field  $\Phi_{\text{full}}$  does not wind around the vacuum manifold when restricted to a small sphere centered on the singular point at  $x = \pm d$ . Indeed, on such a small sphere the value of  $\cos \theta$  is always near zero. The solution restricted to a 2-surface can only have nontrivial winding on the vacuum manifold if at some point  $\sin \theta = 0$ , which means that the 2-surface must intersect the  $z$  axis and so extend a distance  $d$  from the singular point. In fact, the kinetic energy diverges along the infinite lines extending

along the  $z$  axis from the two singular points, which leads to a short-distance logarithmic divergence in the energy.

This divergence is simply an artifact of our simple functional form (3.3). In Appendix A and in Sec. 5, when we consider true solutions of the equations of motion, the field configurations will be regular everywhere and so will the energy be. However, in the present section we are only interested in the interactions between monopoles. What we will do is to subtract off a counter term, which cancels the divergence. We will call this difference the interaction energy and it is free from short-distance divergences. A concern may be that the exact form of the counter term may change the functional behavior of the interaction energy; however, to leading order in  $d$  it is independent of the counter term. To see this, we define the following interaction potential

$$E_{\text{int}} \equiv E[\Phi_{\text{full}}] - E[\Phi_1] - E[\Phi_2], \quad (3.5)$$

where  $\Phi_i$  is the  $i$ -th single monopole which we subtract off

$$\Phi_i = h \{ \sin \theta \cos \phi_i, \sin \theta \sin \phi_i, \cos \theta \}. \quad (3.6)$$

The single monopoles that are subtracted have the same two lines of divergences at  $x = \pm d, y = 0$  and so the respective contributions of their short-distance divergences to the interaction energy cancel. The interaction energy is sufficient to determine the radial force between two monopoles, which is simply its derivative with respect to  $d$ .



The interaction energy is

$$\begin{aligned}
\frac{E_{\text{int}}}{v^2} &= -\frac{1}{2} \int_{\rho \leq L, |z| < L} d^3x \frac{d^4 - 2d^2[x^2 - y^2 \mp (y^2 + x^2)] + (1 \mp 2)(x^2 + y^2)^2}{[(d-x)^2 + y^2][(d+x)^2 + y^2](x^2 + y^2 + z^2)} \\
&= -\int_0^L d\rho \int_0^{2\pi} d\phi \frac{d^4 \pm 2d^2\rho^2 + (1 \mp 2)\rho^4 - 2d^2\rho^2 \cos 2\phi}{d^4 + \rho^4 - 2d^2\rho^2 \cos 2\phi} \arctan\left(\frac{L}{\rho}\right) \\
&= -2\pi \int_0^L d\rho \left(1 \pm \text{sign}(d-\rho) \frac{2\rho^2}{d^2 + \rho^2}\right) \arctan\left(\frac{L}{\rho}\right) \\
&= -\frac{1 \mp 2}{2} \pi(\pi + 2 \log 2)L \mp 8\pi d \arctan \frac{L}{d} \pm 2\pi^2 d \arctan \frac{2dL}{L^2 - d^2} \\
&\quad \mp 4\pi L \log\left(1 + \frac{d^2}{L^2}\right) \mp 4\pi d \log 2 \log \frac{L+d}{L-d} \\
&\quad \pm \frac{1}{2} \pi d \text{Li}_2 \left[-\left(\frac{d-L}{d+L}\right)^2\right] \mp \frac{1}{2} \pi d \text{Li}_2 \left[-\left(\frac{d+L}{d-L}\right)^2\right] \pm \pi d \text{Li}_2 \frac{d+L}{d-L} \\
&\quad \mp \pi d \text{Li}_2 \frac{d-L}{d+L} \pm \pi d \Re \text{Li}_2 \frac{(d+L)(d+iL)}{(d-L)(d-iL)} \mp \pi d \Re \text{Li}_2 \frac{(d-L)(d+iL)}{(d+L)(d-iL)} \\
&= -\frac{1 \mp 2}{2} \pi(\pi + 2 \log 2)L \mp 4\pi^2 d + \mathcal{O}\left(\frac{d^2}{L}\right).
\end{aligned} \tag{3.7}$$

The domain of integration here is chosen, for convenience, to be a cylinder (as opposed to a sphere). The first term in the linear expansion does depend on the geometry of the integration region (cylinder versus sphere etc.), however the second term, corresponding to the force does not. Again the upper sign is for the monopole-monopole case and the lower sign is for the monopole-anti-monopole case.

The mutual force between the monopole and the (anti-)monopole for small  $d$  is

$$\frac{1}{v^2} F_{\text{int}} \simeq \pm 4\pi^2, \tag{3.8}$$

and so the two monopoles (monopole-anti-monopole) repel (attract).

Fig. 2 shows the interaction energies for both cases of type A.

### 3.2 Type B

The next case is a charge-two monopole where  $k$  only winds once and  $g$  winds twice [7]

$$\Phi_{\text{full}} = h \{ \sin(\theta_1 + \theta_2) \cos \phi, \epsilon \sin(\theta_1 + \theta_2) \sin \phi, \cos(\theta_1 + \theta_2) \}, \tag{3.9}$$

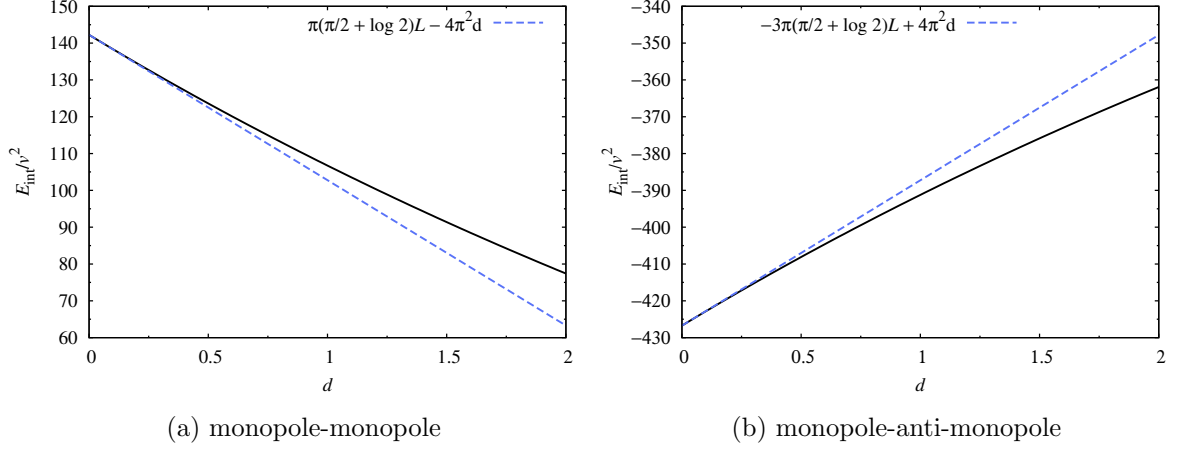


Figure 2: Interaction energy of (a) the type A monopole-monopole pair and (b) the type A monopole-anti-monopole pair as a function of separation distance  $2d$  for a cut-off value  $L = 20$ . The blue dashed line shows linear expansions in  $d$ .

where we define the angles as

$$\theta_1 = \arccos \frac{z-d}{\sqrt{x^2 + y^2 + (z-d)^2}}, \quad \theta_2 = \arccos \frac{z+d}{\sqrt{x^2 + y^2 + (z+d)^2}}, \quad \phi_1 = \arctan \frac{y}{x}, \quad (3.10)$$

and the monopole charges are separated again by a distance  $2d$ .  $\epsilon$  is the twist function; if  $\epsilon = 1$  the configuration describes a monopole-anti-monopole pair, which was considered in Ref. [7]. In order to get a charge-two monopole configuration, we need to twist the second cycle in  $g$ , i.e.,

$$\epsilon = (-1)^{\lfloor \frac{2\theta}{\pi} \rfloor}, \quad (3.11)$$

where  $\lfloor x \rfloor$  is the floor function of  $x$  and

$$\theta = \arccos \frac{z}{\sqrt{x^2 + y^2 + z^2}}, \quad (3.12)$$

is  $\theta$  measured from the origin which is the midpoint between the two monopoles.

Let us now study the point-charge approximation, where  $h := 1$ . We again use the interaction potential (3.5) and  $\Phi_i$ , which is the  $i$ -th monopole, is now given by

$$\Phi_i = h \{ \sin \theta_i \cos \phi, \sin \theta_i \sin \phi, \cos \theta_i \}. \quad (3.13)$$

The interaction energy thus reads

$$\begin{aligned}
\frac{1}{v^2} E_{\text{int}} &= -2 \int_{r \leq L} d^3x \frac{d^2 - z^2}{(d^2 + r^2)^2 - 4d^2 z^2} \\
&= \frac{\pi}{2d} \int_{-L}^L dz \frac{d^2 - z^2}{z} \left[ \log \frac{(d - z)^2}{(d + z)^2} + \log \frac{d^2 + L^2 + 2dz}{d^2 + L^2 - 2dz} \right] \\
&= -\frac{\pi L}{2} \left( \frac{L^2}{d^2} - 3 + \frac{2\pi^2 d}{L} \right) + \frac{\pi L}{2} \left( \frac{L^3}{d^3} + \frac{2L}{d} - \frac{3d}{L} \right) \text{arctanh} \left( \frac{d}{L} \right) \\
&\quad + 2\pi d \eta \left( \frac{d}{L} \right) + \pi d \eta \left( \frac{2dL}{d^2 + L^2} \right) \\
&= \frac{8\pi L}{3} - d\pi^3 + \mathcal{O} \left( \frac{d^2}{L} \right), \tag{3.14}
\end{aligned}$$

where

$$\eta(x) \equiv \text{Li}_2(x) - \text{Li}_2(-x), \tag{3.15}$$

and  $\text{Li}_2$  is the Spence function (also called dilogarithm). Note that the negative sign in front of the order  $d$  term in the expansion means that the system has negative binding energy and the mutual force is repulsive

$$\frac{1}{v^2} F_{\text{int}} \simeq \pi^3. \tag{3.16}$$

Note that the interaction energy remains the same for both the case with the twist function (the monopole-monopole case) and without the twist function (the monopole-anti-monopole case).

In Fig. 3 is shown the interaction energy of the charge-two monopole (which is the same as the monopole-anti-monopole) of type B.

Let us mention that this configuration has no lines of divergences, so only the singular points at the origins of the charges are still present in  $\Phi_{\text{full}}$  but  $E_{\text{int}}$  is again free from these singularities.

We will now consider the total energy, which is the same for both the monopole-

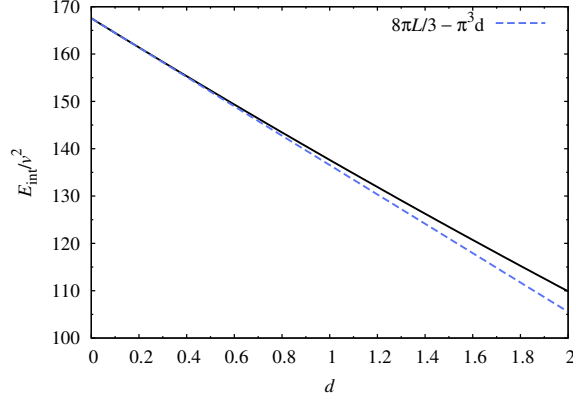


Figure 3: Interaction energy of the type B monopole-monopole pair (which is the same as the type B monopole-anti-monopole) as a function of separation distance  $2d$  for a cut-off value  $L = 20$ . The blue dashed line shows the linear expansion in  $d$ .

monopole and monopole-anti-monopole case,

$$\begin{aligned}
\frac{E_{\text{total}}}{v^2} &= 2 \int_{r \leq L} d^3x \frac{r^2 + z^2}{(d^2 + r^2)^2 - 4d^2z^2} \\
&= \int_{-L}^L \frac{dz}{z} \left[ (d^2 - z^2 - 2dz) \log \frac{(d-z)^2}{d^2 + L^2 - 2dz} + (d^2 - z^2 + 2dz) \log \frac{(d+z)^2}{d^2 + L^2 + 2dz} \right] \\
&= -\frac{\pi L}{2} \left( \frac{L^2}{d^2} - 11 + \frac{2\pi^2 d}{L} \right) + \frac{\pi L}{2} \left( \frac{L^3}{d^3} + \frac{10L}{d} - \frac{11d}{L} \right) \text{arctanh} \left( \frac{d}{L} \right) \\
&\quad + 2\pi d \eta \left( \frac{d}{L} \right) + \pi d \eta \left( \frac{2dL}{d^2 + L^2} \right) \\
&= \frac{32\pi L}{3} - d\pi^3 + \mathcal{O} \left( \frac{d^2}{L} \right). \tag{3.17}
\end{aligned}$$

Again the total energy  $E[\Phi_{\text{full}}]$  diverges linearly in  $L$  for both configurations.

### 3.3 Type C

The last case, which we consider for completeness, is a monopole-anti-monopole where  $k$  winds once and  $g$  winds and unwinds at spatially separate locations [7]

$$\Phi_{\text{full}} = h \{ \sin(\theta_1 - \theta_2) \cos \phi, \sin(\theta_1 - \theta_2) \sin \phi, \cos(\theta_1 - \theta_2) \}, \tag{3.18}$$

where the angles are given in Eq. (3.10) and the monopole and anti-monopole charges are separated again by a distance  $2d$ . This configuration was also considered in Ref. [7].

We again use the point-charge approximation where  $h := 1$ . The interaction potential is given in Eq. (3.5) and the single monopole fields are the same as in Eq. (3.13). The interaction energy thus is

$$\begin{aligned}
\frac{1}{v^2} E_{\text{int}} &= 2 \int_{r \leq L} d^3x \frac{d^2 - r^2}{(d^2 + r^2)^2 - 4d^2 z^2} \\
&= \pi \int_{-L}^L \frac{dz}{z} \left[ (z - d) \log \frac{(z - d)^2}{d^2 + L^2 - 2dz} + (z + d) \log \frac{(z + d)^2}{d^2 + L^2 + 2dz} \right] \\
&= -\frac{\pi(L^2 - d^2)}{d} \log \frac{(d + L)^2}{(d - L)^2} - 4\pi L + 2\pi^3 d - 4\pi d \eta \left( \frac{d}{L} \right) - 2\pi d \eta \left( \frac{2dL}{d^2 + L^2} \right) \\
&= -8\pi L + 2d\pi^3 + \mathcal{O} \left( \frac{d^2}{L} \right). \tag{3.19}
\end{aligned}$$

Note that the positive sign in front of the order  $d$  term in the expansion means that the system has a positive binding energy and the mutual force is attractive

$$\frac{1}{v^2} F_{\text{int}} \simeq -2\pi^3. \tag{3.20}$$

In Fig. 4 is shown the interaction energy of the monopole-anti-monopole of type C.

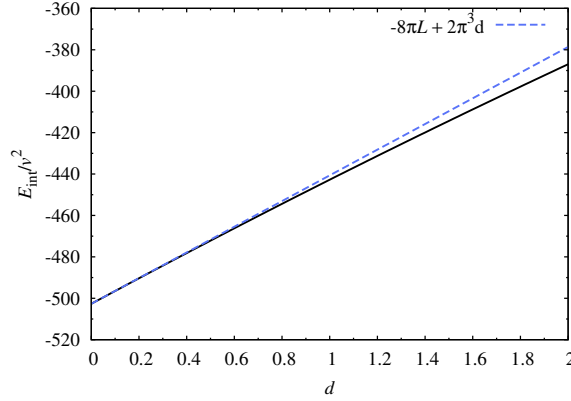


Figure 4: Interaction energy of the type C monopole-anti-monopole as a function of separation distance  $2d$  for a cut-off value  $L = 20$ . The blue dashed line shows the linear expansion in  $d$ .

Finally, we will evaluate the total energy for the type C monopole-anti-monopole

$$\begin{aligned}
\frac{1}{v^2} E_{\text{total}} &= 4d^2 \int_{r \leq L} d^3x \frac{1}{(r^2 + d^2)^2 - 4d^2 z^2} \\
&= \pi d \int_{-L}^L \frac{dz}{z} \left[ \log \frac{(d+z)^2}{(d-z)^2} + \log \frac{d^2 + L^2 - 2dz}{d^2 + L^2 + 2dz} \right] \\
&= 2\pi^3 d - 4\pi d \eta \left( \frac{d}{L} \right) - 2\pi d \eta \left( \frac{2dL}{d^2 + L^2} \right) \\
&= 2d\pi^3 + \mathcal{O} \left( \frac{d^2}{L} \right). \tag{3.21}
\end{aligned}$$

Notice that this and only this case (of those considered here) has a finite total energy.

Let us finally mention that the interaction energy is regular in this case but has a linear divergence in the integral (the constant), whereas the total energy has 2 singular points at the monopole charges but has a finite total energy.

### 3.4 Summary

The conclusion we can draw from the point-charge approximation is that the charge-two monopole is unstable given both orientations we have constructed. The mutual repulsion could be slightly altered by including the profile function  $h$  of the configuration, which in turn includes the effect of the potential. Asymptotically, however, the instability of the global charge-two monopole remains, as we have demonstrated above. For concreteness we carry out a numerical calculation of a perturbed two-monopole configuration in Appendix A to confirm that they are indeed unstable. In the next section we will begin to contemplate how to stabilize the global two-monopole.

## 4 Caging global monopoles

In this section and in the remainder of this paper, we consider the monopole profile function and hence the full equations of motion. The first attempt at stabilizing the global monopoles is to modify the potential in such a way that it is energetically favorable to remain near the spatial origin of a certain coordinate frame. This origin could then be determined dynamically by a solution to a different sector, which we here for concreteness take to be a one-Skyrmion sector.

In this section, we would like to advocate that it is not as trivial to realize this idea as one might expect. We consider for concreteness the following theory

$$-\mathcal{L} = \frac{v^2}{2} \text{Tr}(\partial_\mu \Phi)^2 + \frac{\tilde{\lambda} v^4}{4} (1 + n_4)^\alpha (1 - \text{Tr}[\Phi^2])^2, \quad (4.1)$$

where the field  $n_4$  is a component of the Skyrmion sector which obeys the boundary conditions  $n_4(0) = -1$  (at the origin of the coordinate frame) and  $n_4(\infty) \rightarrow 1$ .

The idea is that at the origin, the potential vanishes and hence the contribution to the energy from the potential is minimal when the monopole is situated at the origin. If the monopole tried to get out, it should start to feel the potential growing and thus it would be energetically favorable to return to the origin. The hope is then that by tuning the potential parameters, the two monopoles still prefer to stay at the origin although they are mutually repulsive. There is however a monkey wrench around the corner. Hence, instead of presenting a numerical calculation, let us examine the expectations with a very crude calculation.

Let us assume that the Skyrmion has the size  $L_{\text{sk}}$ , which for all practical purposes here just means that

$$n_4(r) = -1 + \frac{2r}{L_{\text{sk}}}, \quad \text{for } r < L_{\text{sk}}, \quad (4.2)$$

and  $r$  is the radial coordinate measured from the origin. Let us further assume that a single monopole has the profile shape  $\Phi^a = \sigma^a r / L_{\text{m}}$  for  $r < L_{\text{m}}$ . We consider the case  $L_{\text{sk}} \gg L_{\text{m}}$ , which is what we would prefer for physical reasons. The repulsive force comes from the kinetic term and was estimated in Sec. 3 to be

$$F_{\text{repulsive}} = -4\pi^2 v^2, \quad (4.3)$$

and the attractive force due to the above potential can be estimated as

$$\begin{aligned} F_{\text{attractive}} &= \partial_d \int d^3x \frac{\tilde{\lambda} v^4}{4} [1 + n_4(d)]^\alpha (1 - \text{Tr}[\Phi^2])^2 \\ &= \frac{2\alpha \tilde{\lambda} v^4}{L_{\text{sk}}} \int dr r^2 \left( \frac{2d}{L_{\text{sk}}} \right)^{\alpha-1} \left( 1 - \frac{r^2}{L_{\text{m}}} \right)^2. \end{aligned} \quad (4.4)$$

Since we assumed that the monopole size is much smaller than the size of the Skyrmion ( $L_{\text{m}} \ll L_{\text{sk}}$ ), we can crudely pull the factor of  $(2d/L_{\text{sk}})^{\alpha-1}$  out of the integral and we get

$$F_{\text{attractive}} = \frac{16\alpha\pi\tilde{\lambda}v^4L_{\text{m}}^3}{105L_{\text{sk}}} \left( \frac{2d}{L_{\text{sk}}} \right)^{\alpha-1}. \quad (4.5)$$

Now, the distance from the center of the origin  $d$ , has to be small for the potential to be effective (in the sense of exerting a force on the monopole); that is,  $d < L_{\text{sk}}$ .<sup>1</sup> Let us now compare the forces, i.e. the attractive one versus the repulsive one

$$\frac{4\alpha\tilde{\lambda}v^2L_{\text{m}}^3}{105L_{\text{sk}}}\left(\frac{2d}{L_{\text{sk}}}\right)^{\alpha-1} > \pi. \quad (4.6)$$

The inequality shows that a larger Skymion provides a smaller attractive force (this is also expected as the derivative of the field profile becomes smaller). The real kicker is that by trying to increase the potential factor, i.e.  $\tilde{\lambda}v^2$ , the monopole size decreases by the same factor, namely  $L_{\text{m}}^{-2} \sim \tilde{\lambda}v^2$ . This means that the only parameter we can dial to stabilize the monopole(s) is  $\alpha$ . However, a large value of  $\alpha$  also makes the factor  $(2d/L_{\text{sk}})^{\alpha-1}$  small. In other words, once we try to squeeze in the monopole(s) by the potential, they shrink and can escape as easily as before.

This is not supposed to be a proof of no-go, but merely a justification of not constructing the theory with just a modified potential. We have tried several numerical attempts and have observed exactly this behavior, namely that the monopoles shrink and are able to escape. We do not consider those attempts as a proof of no-go either and will not present this study here. In the next section we will pursue a different strategy.

## 5 Skymopole

In this section we will place a global two-monopole inside a potential so that each monopole will not run away despite mutual repulsion. In view of the estimates of the last section, we consider a coupling between a one-Skymion and the two-monopole via a metric-like prefactor of the monopole part of the Lagrangian density. The aim is that the monopole constituents prefer to stay in the center of the “potential”, so much so that the repulsion is negligible. If a monopole constituent is to exit the Skymion, it will enjoy the instabilities described in the Sec. 3.

Let us first contemplate the construction in order to know what to expect. We start with a Skymion which has a kinetic term, a Skyrme term and a mass term. The size of the Skymion is given by the balance of these three terms. The global monopole, on the other hand, has a size squared given by the inverse coefficient of the self-interacting

---

<sup>1</sup>One may naively think that the factor is helping at making the force bigger when  $d > L_{\text{sk}}/2$ , but in the real Skymion solution, the tail is much flatter at such distances from the origin and hence the derivative becomes small.



potential term. In front of the monopole sector we multiply by a factor depending on the profile of the Skymion sector.

Putting the pieces together gives us the Lagrangian density

$$\mathcal{L} = \mathcal{L}_{\text{sk}} + \mathcal{G}(n_4)\mathcal{L}_{\text{m}} \quad (5.1)$$

where the Skymion Lagrangian is simply

$$-\mathcal{L}_{\text{sk}} = \frac{c_2}{2}(\partial_\mu \mathbf{n} \cdot \partial^\mu \mathbf{n}) + \frac{c_4}{4} [(\partial_\mu \mathbf{n} \cdot \partial^\mu \mathbf{n})^2 - (\partial_\mu \mathbf{n} \cdot \partial_\nu \mathbf{n})^2] + m^2(1 - n_4), \quad (5.2)$$

the monopole Lagrangian reads

$$-\mathcal{L}_{\text{m}} = \frac{v^2}{2} \text{Tr}(\partial_\mu \Phi \partial^\mu \Phi) + \frac{\lambda v^4}{4} (1 - \text{Tr}[\Phi^2])^2, \quad (5.3)$$

and the coupling is chosen to be

$$\mathcal{G}(n_4) = \left( \frac{1 + b + n_4}{2 + b} \right)^\alpha, \quad (5.4)$$

where the fields  $n_p$ , with  $p = 1, \dots, 4$  are unitless  $O(4)$  fields describing the Skymion part of the configuration and  $\Phi = \Phi^a \sigma^a$ ,  $a = 1, 2, 3$  are  $SU(2)$  adjoint unitless monopole fields. The coefficients in the Lagrangians are  $c_2$  and  $m$  with units of mass squared,  $v$  has units of mass, and finally  $c_4$ ,  $\lambda$ ,  $b$  and  $\alpha$  are unitless parameters.  $c_2$ ,  $c_4$  and  $m$  determine the size of the Skymion and  $\sqrt{\lambda}v$  determines the size of the monopole(s).  $b$  is included in order for the monopole energy not to vanish at the center of the Skymion and larger values of  $\alpha$  translate to a larger attractive force among the monopoles. One may interpret the coupling,  $\mathcal{G}$ , as an effective metric felt by the monopole sector of the theory (although here it is just incarnated as a non-renormalizable field theory coupling).

If we compare to the considerations made in the last section, the difference is that now the size of the monopoles and the size of the energy barrier are independent parameters of the theory.

The static equations of motion are

$$c_2 \partial^2 n_p + c_4 (\partial_i \mathbf{n} \cdot \partial_i \mathbf{n}) \partial^2 n_p + c_4 (\partial_i \partial_j \mathbf{n} \cdot \partial_j \mathbf{n}) \partial_i n_p - c_4 (\partial^2 \mathbf{n} \cdot \partial_i \mathbf{n}) \partial_i n_p - \frac{\alpha v^2}{2 + b} \left( \frac{1 + b + n_4}{2 + b} \right)^{\alpha-1} \left[ \frac{1}{2} \text{Tr}(\partial_\mu \Phi)^2 \delta^{p4} + \frac{\lambda v^2}{4} (1 - \text{Tr}[\Phi^2])^2 \right] + m^2 \delta^{p4} = 0, \quad (5.5)$$

$$\partial^2 \Phi + \frac{\alpha}{1 + b + n_4} \partial_\mu n_4 \partial^\mu \Phi^a + \lambda v^2 (1 - \text{Tr}[\Phi^2]) \Phi = 0. \quad (5.6)$$

The vacuum equations are

$$\text{Tr}[\Phi^2] = 1, \quad n_4 = 1. \quad (5.7)$$

Note that even without the mass term for  $\mathbf{n}$ , there is no explicit breaking of  $O(4)$  symmetry, the symmetry is still broken spontaneously down to  $O(3)$  for any finite energy state. This breaking,  $O(4) \rightarrow O(3)$ , supports the Skyrmion(s). The spontaneous breaking of  $SU(2)$  down to  $U(1)$  by the potential supports the monopoles.

There is a subtlety due to the coupling of the monopole theory to the Skyrmion sector in this way, namely that the second last term in Eq. (5.5) cannot exceed the value of the mass term in order for the field,  $n_4$ , to be able to return to its vacuum expectation value. When this is not fulfilled, so-called pion condensation occurs and the vacuum equations are completely different, see e.g. Ref. [11]. This leads to the following (strong) condition:

$$\frac{\alpha v^2}{2+b} \left[ \frac{1}{2} \text{Tr}(\partial_\mu \Phi)^2 + \frac{\lambda v^2}{4} (1 - \text{Tr}[\Phi^2])^2 \right] < m^2, \quad (5.8)$$

where we have neglected the factor of  $((1+b+n_4)/(2+b))^{\alpha-1}$ , as it is always smaller or equal to unity (by construction). This means that the region in parameter space we are interested in is where  $\alpha$  is big (to get a sizable attractive force) and  $v$  is small (to avoid breaking the vacuum conditions).<sup>2</sup>

The Skyrmion charge is also a topological charge and can be calculated as

$$B = -\frac{1}{12\pi^2} \int d^3x \epsilon^{pqrs} \epsilon^{ijk} \partial_i n_p \partial_j n_q \partial_k n_r n_s. \quad (5.9)$$

In order to get a feeling for the parameters in the theory, let us consider a 1-Skyrmion with a single monopole inside, i.e.  $Q = B = 1$ . For this we can choose the following Ansätze

$$\mathbf{n} = \{ \hat{x}^1 \sin f(r), \hat{x}^2 \sin f(r), \hat{x}^3 \sin f(r), \cos f(r) \}, \quad (5.10)$$

$$\Phi = h(r) \hat{x}^a \sigma^a, \quad (5.11)$$

where  $\hat{x}^a = x^a/r$  is the spatial unit vector and  $r = |x|$  is the radial coordinate. Inserting the above into the Lagrangians (5.2) and (5.3), we get

$$-\mathcal{L}_{\text{sk}} = \frac{c_2}{2} f_r^2 + \frac{c_2}{r^2} \sin^2 f + \frac{c_4}{r^2} \sin^2(f) f_r^2 + \frac{c_4}{2r^4} \sin^4 f + m^2(1 - \cos f), \quad (5.12)$$

$$-\mathcal{G}(n_4) \mathcal{L}_{\text{m}} = \left( \frac{1+b+\cos f}{2+b} \right)^\alpha \left[ \frac{v^2}{2} h_r^2 + \frac{v^2}{r^2} h^2 + \frac{\lambda v^4}{4} (1-h^2)^2 \right], \quad (5.13)$$

---

<sup>2</sup>If the boundary conditions are switched so that  $n_4 = 1$  at the origin and  $n_4 = -1$  at spatial infinity, the same condition holds with  $n_4 \rightarrow -n_4$ , i.e. it does not ameliorate the problem.

which give rise to the following equations of motion

$$c_2 \left( f_{rr} + \frac{2}{r} f_r - \frac{1}{r^2} \sin 2f \right) + c_4 \left( \frac{2}{r^2} \sin^2(f) f_{rr} + \frac{1}{r^2} \sin(2f) f_r^2 - \frac{1}{r^4} \sin^2 f \sin 2f \right) - m^2 \sin f + \frac{\alpha v^2}{2+b} \left( \frac{1+b+\cos f}{2+b} \right)^{\alpha-1} \left[ \frac{1}{2} h_r^2 + \frac{1}{r^2} h^2 + \frac{\lambda v^2}{4} (1-h^2)^2 \right] \sin f = 0, \quad (5.14)$$

$$h_{rr} + \frac{2}{r} h_r - \frac{2}{r^2} h - \frac{\alpha \sin f}{1+b+\cos f} f_r h_r + \lambda v^2 (1-h^2) h = 0, \quad (5.15)$$

where  $f_r \equiv \partial_r f$ . Let us now expand the equations of motion around  $r = 0$  as

$$f = \pi + f_1 r + \frac{1}{2} f_2 r^2 + \dots, \quad h = h_1 r + \frac{1}{2} h_2 r^2 + \dots. \quad (5.16)$$

The equations of motion to leading order in  $r$  determine  $f_2 = h_2 = 0$ . We can thus calculate the energy density around the origin as

$$\mathcal{E} = \frac{3}{2} c_2 f_1^2 + \frac{3}{2} c_4 f_1^4 + 2m^2 + \frac{3}{2} v^2 \left( \frac{b}{2+b} \right)^\alpha \left[ h_1^2 + \frac{1}{6} \lambda v^2 \right] + \mathcal{O}(r^2). \quad (5.17)$$

Using instead a scaling argument due to Derrick [12], we can estimate the size of the Skyrmion as follows. Neglecting the monopole fields (as we assume that  $v^2 \ll (c_2, m)$ ), we denote by  $e_{2,4}$  the kinetic energy terms with 2 and 4 derivatives and  $u$  is the unitless potential

$$E = c_2 e_2 + c_4 e_4 + m^2 u. \quad (5.18)$$

Rescaling now the spatial coordinates  $x^i \rightarrow \mu x^i$ , we get

$$E \rightarrow \frac{1}{\mu} c_2 e_2 + \mu c_4 e_4 + \frac{1}{\mu^3} m^2 u, \quad (5.19)$$

which has an equilibrium when

$$\mu^4 c_4 e_4 - \mu^2 c_2 e_2 - 3m^2 u = 0. \quad (5.20)$$

If we neglect the kinetic term, assuming that the mass is big and the size of the Skyrmion is also big, then the characteristic length scale and hence the Skyrmion size is roughly

$$L_{\text{sk}} \sim \sqrt[4]{\frac{c_4}{3m^2}}. \quad (5.21)$$

The final step is to identify  $f_1$  in the expansion of the solution as an order-one number times the inverse length scale:  $f_1 \sim 1/L_{\text{sk}}$ . Now we can write the energy density of the Skyrmion part as

$$\mathcal{E}_{\text{sk}} \sim \frac{3\sqrt{3} c_2 m}{2 \sqrt{c_4}} + 5m^2, \quad (5.22)$$

whereas the energy density of the monopole part is roughly

$$\mathcal{E}_{\text{m}} \sim \frac{1}{2} \lambda v^4 \left( \frac{b}{2+b} \right)^\alpha. \quad (5.23)$$

## 5.1 A single Skyrmopole

Let us try to solve the coupled equations numerically. We use the finite-difference method on a cubic lattice of sizes  $121^3$  and  $201^3$  and evolve a linear time operator, which is standard in the relaxation method.<sup>3</sup> After the equations of motion are satisfied locally better than the one-permille level we stop the relaxation algorithm. We use the Ansätze (5.10)-(5.11) with appropriate radial profile functions as the initial configuration for the relaxation algorithm. We have chosen the parameters as  $c_2 = 1$ ,  $c_4 = 4$ ,  $m = 1$ ,  $v = 1/4$ ,  $\lambda = 128$ ,  $b = 1/2$  and  $\alpha = 4$  in order to satisfy the constraint (5.8). In Fig. 5 is shown a single global monopole ( $Q = 1$ ) inside a single Skyrmion ( $B = 1$ ). The figure shows the 3-dimensional isosurfaces of the Skyrmion charge and monopole charge densities, respectively, each at their respective half-maximum values.

The size and density (lattice spacing) is the same as that used for the two-monopole inside a Skyrmion and we have optimized said dimensions for the two-monopole. This is why we do not capture the  $Q = 1$  monopole charge better than to about three and a half percent on this lattice. As we will see shortly, the two-monopole charge is far better contained.

In Fig. 6 are shown  $xy$  slices at  $z = 0$  of the monopole charge and Skyrmion charge, respectively. Both have the shape of solid balls and the monopole has roughly half the diameter of that of the Skyrmion.

In Fig. 7 are shown six  $xy$  slices at  $z = 0$  of energy densities. More precisely of the monopole kinetic energy, the Skyrmion kinetic energy, the monopole potential, the pion mass term (Skyrmion potential), the total energy and finally the logarithm of the total energy. The shape of the Skyrmion is ball-like while that of the monopole is rather like a hollow sphere. This is in contradistinction to the monopole charge-density distribution. The reason is that the monopole energy is multiplied by a factor  $\mathcal{G}$ , which amplifies the energy outside of where the monopole charge is located. This is no accident. This is made by design of the function  $\mathcal{G}$  in order to provide an attractive force on the two monopole constituents. One can think of this construction as making an energy barrier that the monopoles do not want to cross and hence choose to stick with each other instead (even though they are repellent to one another).

The reason why this calculation is so numerically challenging is that the monopole

---

<sup>3</sup>Clearly, the single Skyrmpole case,  $Q = B = 1$ , can be solved using just the ordinary differential equations and not the three-dimensional partial differential equations (PDEs). In fact we solved this case also using an ODE solver and compared the solution to the one shown here found by solving the PDE as a check on our code.

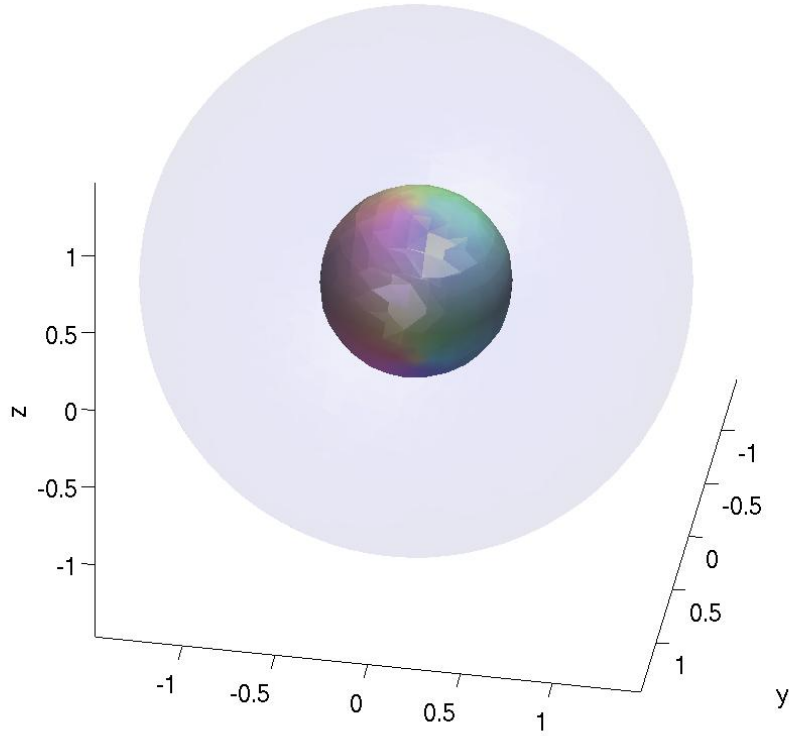


Figure 5: A global monopole inside a Skymion. The figure shows isosurfaces of the monopole charge and Skymion charge densities, respectively, at half their respective maximum values. The gray cloud is the Skymion charge isosurface and the colored isosurface is the monopole charge. The coloring is made using an HSL (hue-saturation-lightness) map from the monopole field such that  $\arg(\Phi_1/\Phi_2)$  is mapped to the hue and  $|\Phi_3|$  determines the lightness. The parameters are chosen as:  $c_2 = 1$ ,  $c_4 = 4$ ,  $m = 1$ ,  $v = 1/4$ ,  $\lambda = 128$ ,  $b = 1/2$  and  $\alpha = 4$ , and the numerically integrated charges are  $B = 0.99993$  and  $Q = 0.96707$ . The calculation is made on a  $201^3$  cubic lattice.

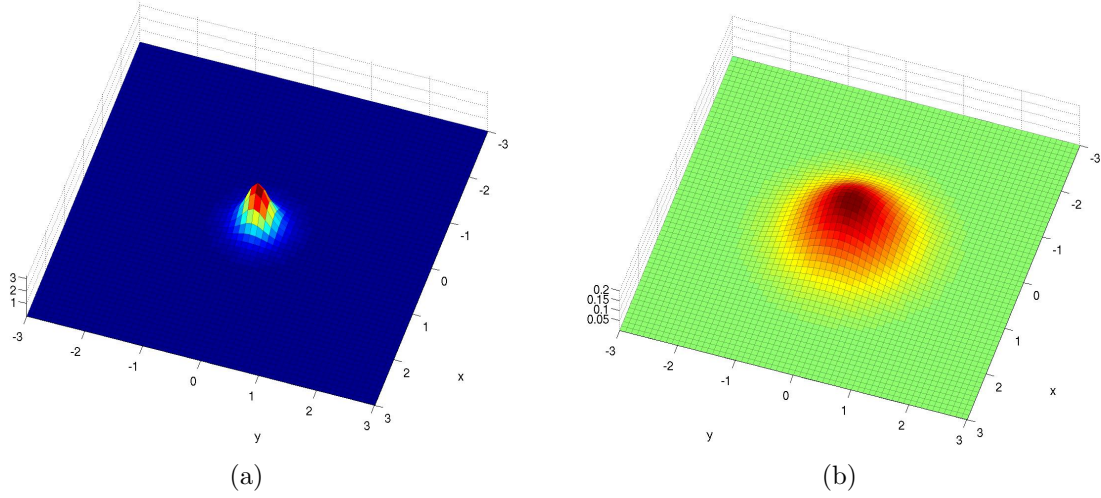


Figure 6: Topological charges for the global monopole inside a Skyrmion; (a) is the monopole charge and (b) is the Skyrmion charge. The figures show slices in the  $xy$  plane for  $z = 0$ . The numerically integrated charges are  $B = 0.99993$  and  $Q = 0.96707$ .

charge is much smaller than the corresponding energy distribution. This is because the prefactor makes the majority of the monopole energy density sit outside of where the monopole charge is situated. This separation of scales requires both very large length scales (for capturing the energy) and a very dense lattice for capturing the charge at the center.

## 5.2 The type A, $Q = 2$ Skyrmpole

We are now ready to compute the two-monopole inside a single Skyrmion; we can call it the  $Q = 2$  Skyrmpole. As the initial condition we use the Ansätze (5.10) and (3.3) with  $d = 0$ . We take the profile function of the initial condition to be

$$h = \tanh[\kappa r],$$

where  $r$  is the radial coordinate and  $\kappa$  is an appropriately chosen constant. We use the same lattice and same parameters as in the previous subsection, i.e.  $c_2 = 1$ ,  $c_4 = 4$ ,  $m = 1$ ,  $v = 1/4$ ,  $\lambda = 128$ ,  $b = 1/2$  and  $\alpha = 4$ . We again satisfy the constraint (5.8). In Fig. 8 is shown the global two-monopole ( $Q = 2$ ) inside a single Skyrmion ( $B = 1$ ). The figure shows the 3-dimensional isosurfaces of the Skyrmion charge and monopole charge densities, respectively, each at their respective half-maximum values.

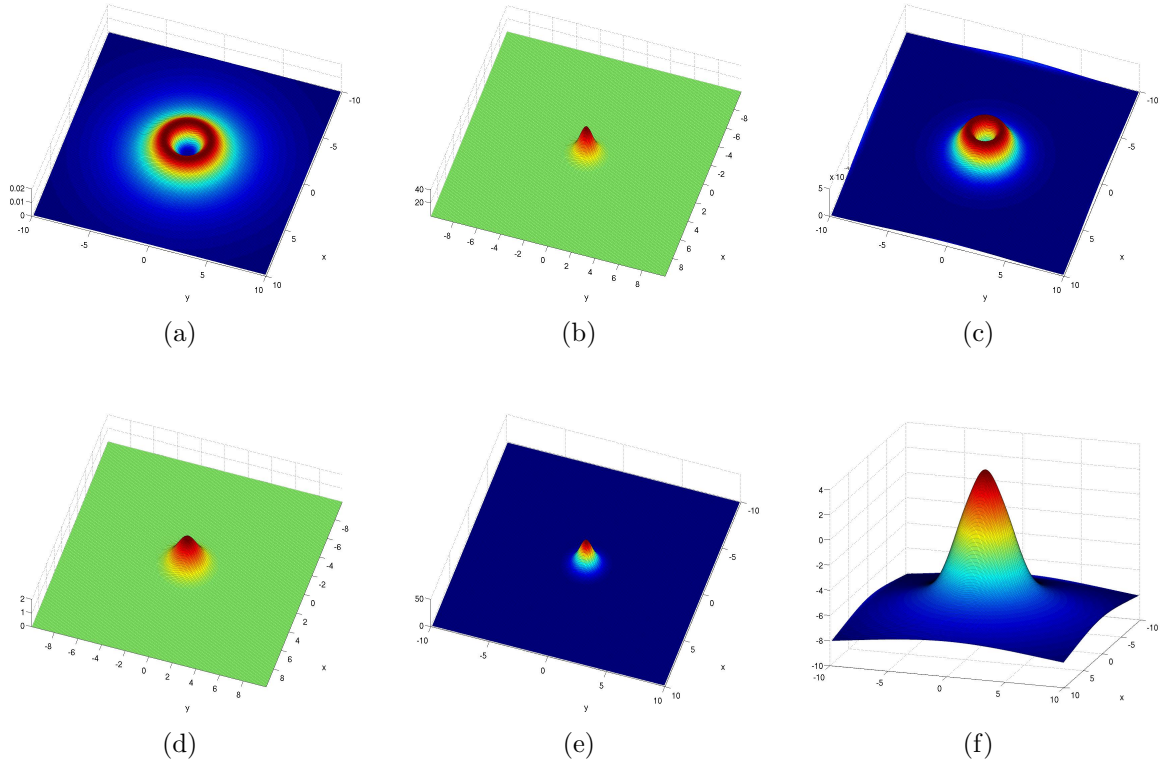


Figure 7: Energies for the global monopole inside a Skymion; (a) is the kinetic term of the monopole (with the prefactor  $\mathcal{G}$ ), (b) is the Skymion kinetic energy, (c) is the potential for the monopole (again with the prefactor  $\mathcal{G}$ ), (d) is the pion-mass term of the Skymion sector, (e) is the total energy of the configuration and (f) is the logarithm of the total energy. The figures show slices in the  $xy$  plane for  $z = 0$ .

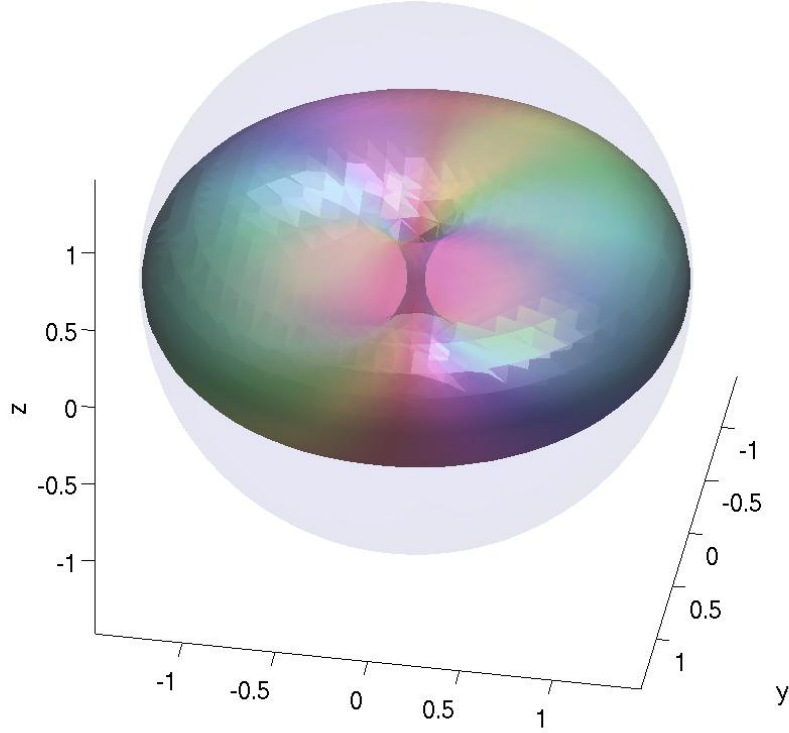


Figure 8: The global two-monopole of type A inside a single Skyrmin. The figure shows isosurfaces of the monopole charge and Skyrmin charge densities, respectively, at half their respective maximum values. The gray cloud is the Skyrmin charge isosurface and the colored isosurface of the shape of a torus is the monopole charge. The coloring is made using an HSL (hue-saturation-lightness) map from the monopole field such that  $\arg(\Phi_1/\Phi_2)$  is mapped to the hue and  $|\Phi_3|$  determines the lightness. The parameters are chosen as:  $c_2 = 1$ ,  $c_4 = 4$ ,  $m = 1$ ,  $v = 1/4$ ,  $\lambda = 128$ ,  $b = 1/2$  and  $\alpha = 4$ , and the numerically integrated charges are  $B = 0.99993$  and  $Q = 1.9863$ . The calculation is made on a  $201^3$  cubic lattice.



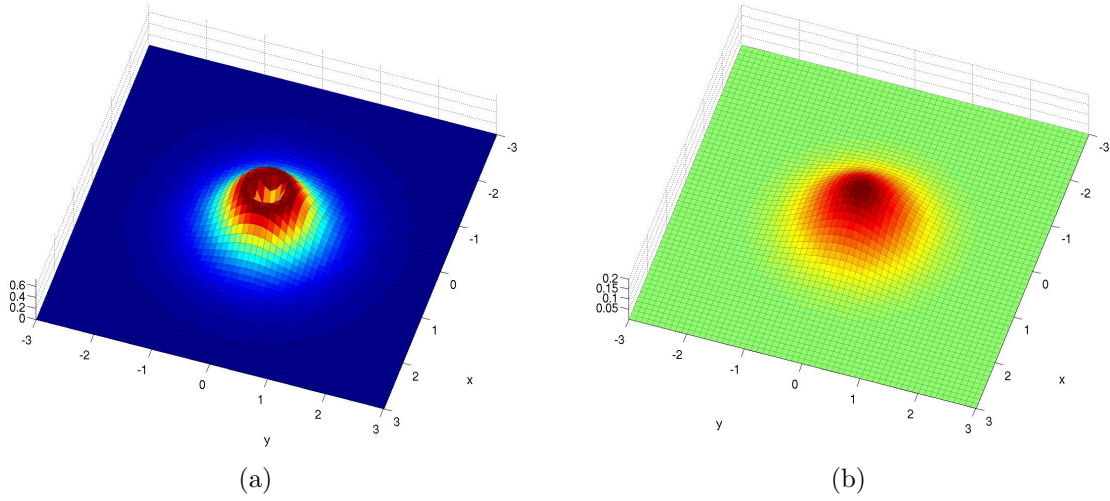


Figure 9: Topological charges for the global two-monopole inside a single Skyrmion; (a) is the monopole charge and (b) is the Skyrmion charge. The figures show slices in the  $xy$  plane for  $z = 0$ . The numerically integrated charges are  $B = 0.99993$  and  $Q = 1.9863$ .

In Fig. 9 are shown  $xy$  slices at  $z = 0$  of the monopole charge and Skyrmion charge, respectively. The Skyrmion is still a ball while the charge distribution of the two-monopole has the shape of a torus. Notice that the two charge distributions have almost the same size.

In Fig. 10 are shown six  $xy$  slices at  $z = 0$  of energy densities. Again the subfigures show the monopole kinetic energy, the Skyrmion kinetic energy, the monopole potential, the pion mass term (Skyrmion potential), the total energy and finally the logarithm of the total energy. As was the case of the shapes in the one-monopole case, the Skyrmion energy is ball-like while the monopole energy has the shape of a hollow sphere.

We numerically integrate the energy densities shown in Fig. 10 and give the results in Tab. 1. We integrate only the solution inside the box on which we find the solution, which has the size  $20^3$ . This captures the total energy of the Skyrmion, whereas the total energy of the two-monopole is infinite.

### 5.3 Stability of the type A, $Q = 2$ Skyrmpole

A caveat of starting with a symmetric initial condition is that it may be unstable and only a very long relaxation time will reveal if the configuration is really stable or not.

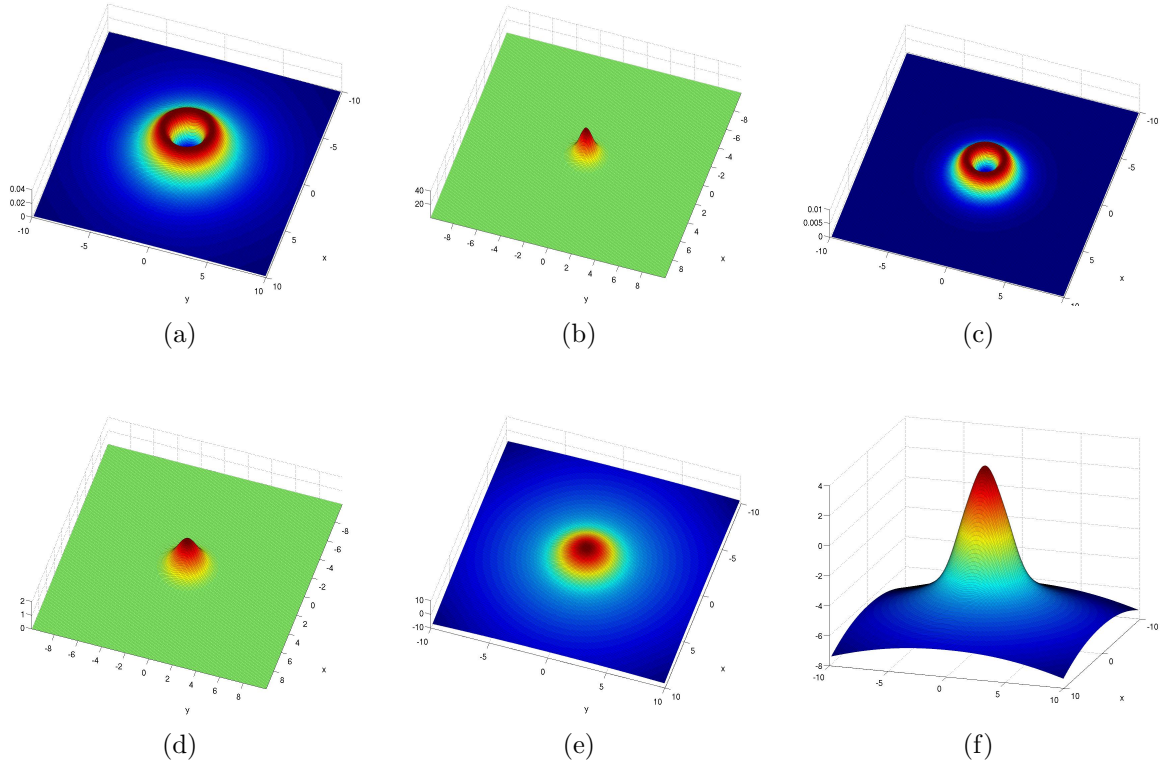


Figure 10: Energies for the global two-monopole inside a single Skyrmion; (a) is the kinetic term of the monopole (with the prefactor  $\mathcal{G}$ ), (b) is the Skyrmion kinetic energy, (c) is the potential for the monopole (again with the prefactor  $\mathcal{G}$ ), (d) is the pion-mass term of the Skyrmion sector, (e) is the total energy of the configuration and (f) is the logarithm of the total energy. The figures show slices in the  $xy$  plane for  $z = 0$ .

Table 1: Numerically integrated energies of the type A,  $Q = 2$  Skyrmpole. The integration region is the box on which the discretized solution is found, which has the size  $20^3$ .

monopole kinetic energy	$16.18 \pm 0.11$
Skyrmion kinetic energy	$166.99 \pm 0.17$
monopole potential energy	$0.28 \pm 0.002$
Skyrmion potential energy	$25.49 \pm 0.03$
total energy	$208.88 \pm 0.21$

In our case of the type A two-monopole, the symmetry enjoyed by the configuration is axial symmetry. In order to show that the system of the two-monopole residing within the Skyrmion is really stable, we use again the Ansätze (5.10) and (3.3), but this time we perturb the axial symmetry by a finite  $d > 0$  parameter. More specifically, we choose

$$d = \frac{1}{2} a h_x, \quad (5.24)$$

where  $a$  is a real number and  $h_x$  is the lattice spacing in the  $x$  direction. We carry out this calculation on a  $121^3$  lattice with spatial-lattice spacing  $h_x = h_y = h_z = 0.16529$ . Since the winding phases now have two centers – one at  $x = -d$  and one at  $x = d$ , we choose a profile function of the form

$$h = \sqrt{\tanh \left[ \kappa ((x - d)^2 + y^2 + z^2)^{\frac{3}{8}} \right] \tanh \left[ \kappa ((x + d)^2 + y^2 + z^2)^{\frac{3}{8}} \right]}, \quad (5.25)$$

with an appropriate value for  $\kappa > 0$ . The fractional power of the radius in the hyperbolic tangent is chosen empirically to better match the  $d = 0$  solution. In order to quantify the asymmetry of the configuration, we define the following spatially-weighted monopole charge

$$Q_{x^i} \equiv \int d^3x \, x^i \mathcal{Q}, \quad (5.26)$$

where the monopole charge density is

$$\mathcal{Q} = -\frac{1}{8\pi} \epsilon^{ijk} \epsilon^{abc} \partial_i \Phi^a \partial_j \Phi^b \partial_k \Phi^c. \quad (5.27)$$

In Fig. 11 is shown the asymmetry between the monopole charge distribution in the  $x$  and the  $y$  direction for various deformation values  $a = 1, \dots, 5$  as function of relaxation time  $\tau$ . In the shown relaxation-time interval, all the configurations clearly converge

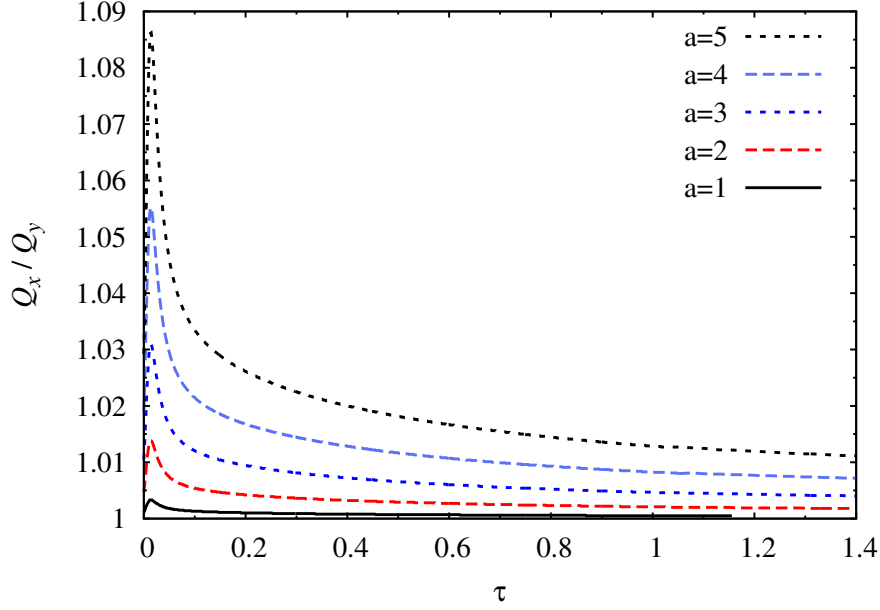


Figure 11: Asymmetry in the monopole charge,  $Q_x/Q_y$  as function of relaxation time  $\tau$ , for various values of the deformation parameter  $a$ .

towards the non-deformed configuration, i.e.  $d = 0$ . The more deformed the initial configuration is, the longer it takes for the relaxation to relax the configuration back to the non-deformed one.

In Fig. 12 is shown a series of snapshots of the isosurfaces of Skyrmion and monopole charges as the relaxation time progresses. This particular series is made with the deformation parameter  $a = 5$ . The configuration quickly converges towards a torus shape and after a sufficiently long relaxation time, it becomes infinitesimally close to the  $a = 0$  ( $d = 0$ ) solution.

In Fig. 13 is shown a series of snapshots of the contours of the norm of the monopole field

$$\sqrt{(\Phi^1)^2 + (\Phi^2)^2 + (\Phi^3)^2}. \quad (5.28)$$

as the relaxation time progresses. This particular series is again made with the deformation parameter  $a = 5$ . It is observed from the innermost contour(s) that the monopole field possesses two zeros when the relaxation algorithm begins. After the time of Fig. 13f and before Fig. 13g, the two zeros merge to a single zero and hence becomes the non-deformed solution  $a = 0$  ( $d = 0$ ). We take this as a proof of stability of the torus-like solution shown in the last subsection.

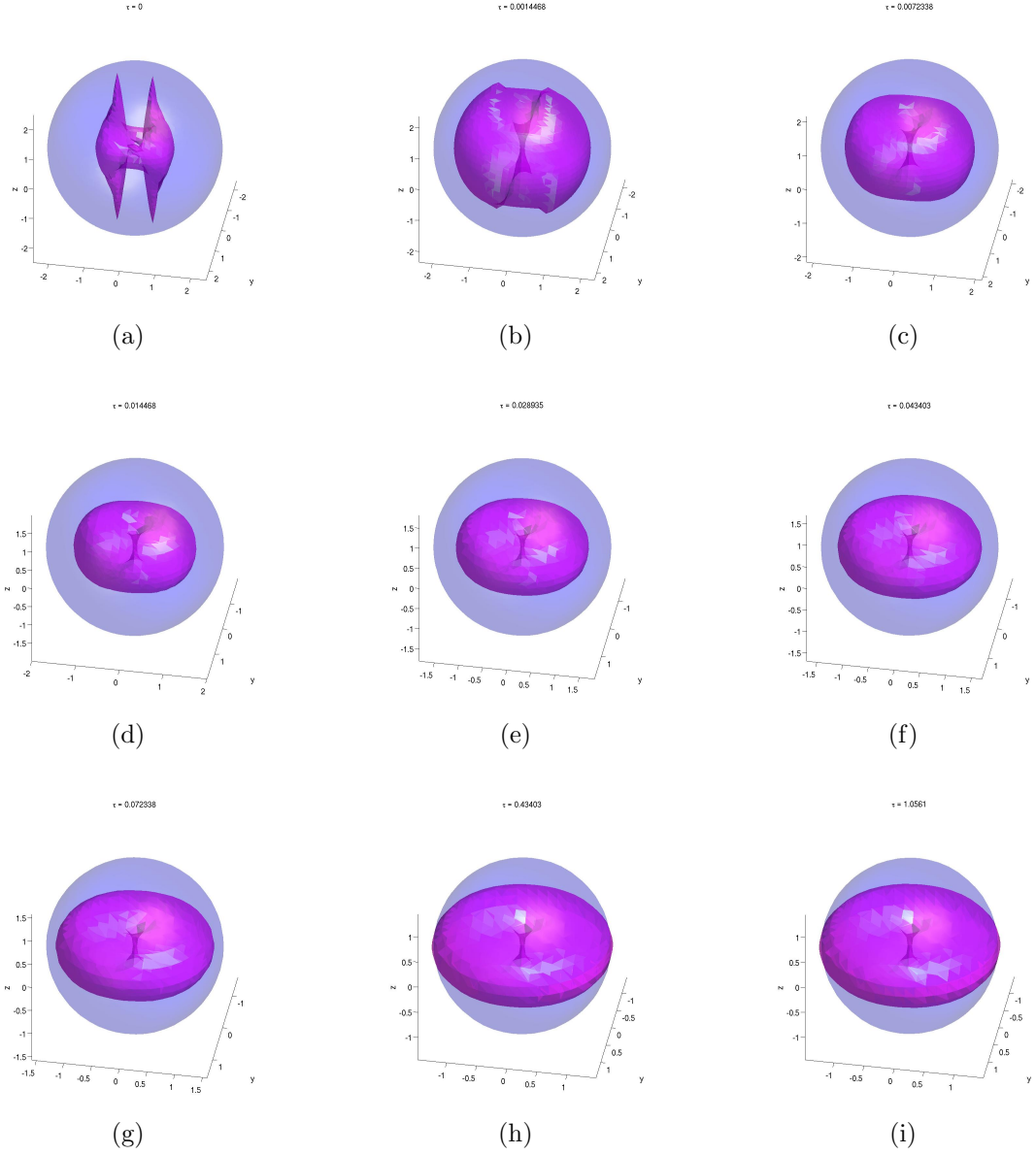


Figure 12: The global two-monopole with a deformed initial condition ( $a = 5$ ) inside a single Skyrmion. The figures show isosurfaces of the monopole charge and Skyrmion charge densities, respectively, at half their respective maximum values. The blue surface is the Skyrmion charge and the magenta surface is the monopole charge. As the relaxation time progresses, the solution converges towards that of Fig. 8. The calculation is made on a  $121^3$  cubic lattice.

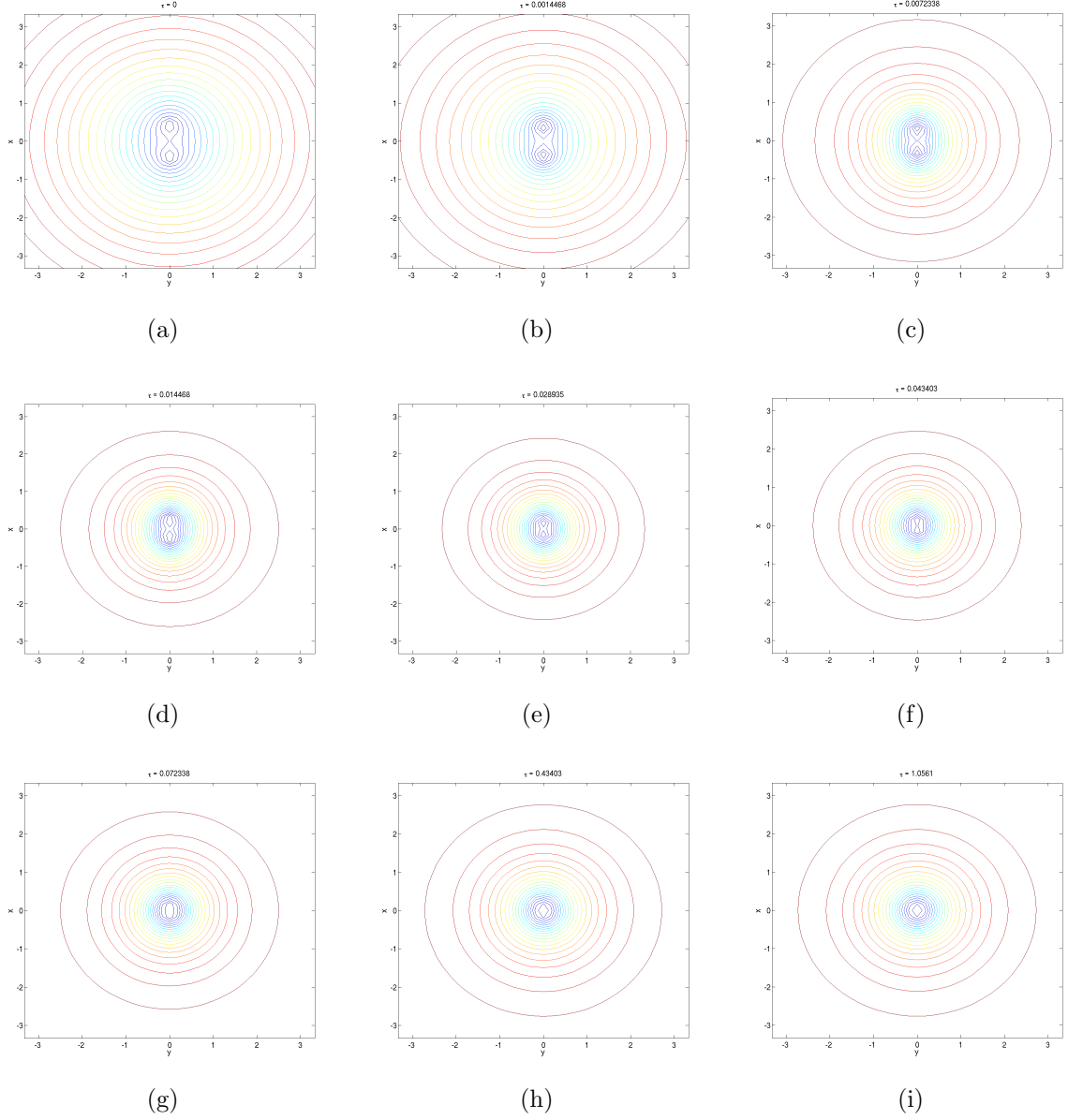


Figure 13: The global two-monopole with a deformed initial condition ( $a = 5$ ) inside a single Skyrmion. The figures show contours of the norm of  $\Phi$ , i.e.  $\sqrt{\Phi_1^2 + \Phi_2^2 + \Phi_3^2}$  on an  $xy$  slice at  $z = 0$ . The blue circles in the middle of figures (a)-(f) show two separated zeros in the monopole field. As the relaxation time progresses, the two distinct zeros clearly merge to a single zero and the solution converges towards that of Fig. 8.

## 5.4 Instability of the type B, $Q = 2$ Skyrmopole

Although we find that the type A,  $Q = 2$  Skyrmopole of Sec. 5.2 is stable for the chosen values of the parameters in the model, we also find that the corresponding type B,  $Q = 2$  Skyrmopole is less stable. We carry out the same calculation as in Sec. 5.2, but with the initial condition given by the Ansätze (5.10) and (3.9) with  $d = 0$  and the parameters are again chosen as  $c_2 = 1$ ,  $c_4 = 4$ ,  $m = 1$ ,  $v = 1/4$ ,  $\lambda = 128$ ,  $b = 1/2$  and  $\alpha = 4$ . We take the profile function of the initial condition to be

$$h = \tanh[\kappa r],$$

where  $r$  is the radial coordinate and  $\kappa$  is an appropriately chosen constant. We find that for this choice of parameters, the type B configuration is unstable. In Fig. 14 is shown a series of snapshots of the isosurfaces of Skyrmion and monopole charges as the relaxation time progresses. We observe that the two monopole constituents split up, escape the Skyrmion and move off to infinity. This is, however, by no means a proof that the type B configuration cannot be stabilized. We suspect however, that by tuning the parameters to stabilize the type B configuration, it will eventually converge to the solution of type A.

## 6 Conclusion

In this paper we have shown that the two-monopole is unstable by itself both in the point-charge approximation and with a smooth profile function on a cubic lattice. In order to stabilize the two-monopole we first considered adding an interaction term to the monopole Lagrangian, but pointed out the difficulties in such an approach. For this reason we followed a different path to stabilize it. The strategy is to create an energy barrier for the monopoles to overcome in order for them to escape a spatial region. This energy barrier was created as an example by a function that multiplies the entire monopole Lagrangian and interpolates between a low value in the center of the region where the monopoles are to be contained and a high value outside. We have shown with a given set of parameters, the two-monopole is stable when the initial guess is of type A and by perturbing said configuration, we have further shown that it returns to the found solution after a sufficient amount of relaxation time.

This type of stable solution has one feature which, for some purposes, may be undesirable. Namely, that the Skyrmion energy density dominates the monopole one on the scales of the charges. Of course the two-monopole has a diverging total energy as it is a global type of monopole, while the Skyrmion has a finite total energy. It may be possible

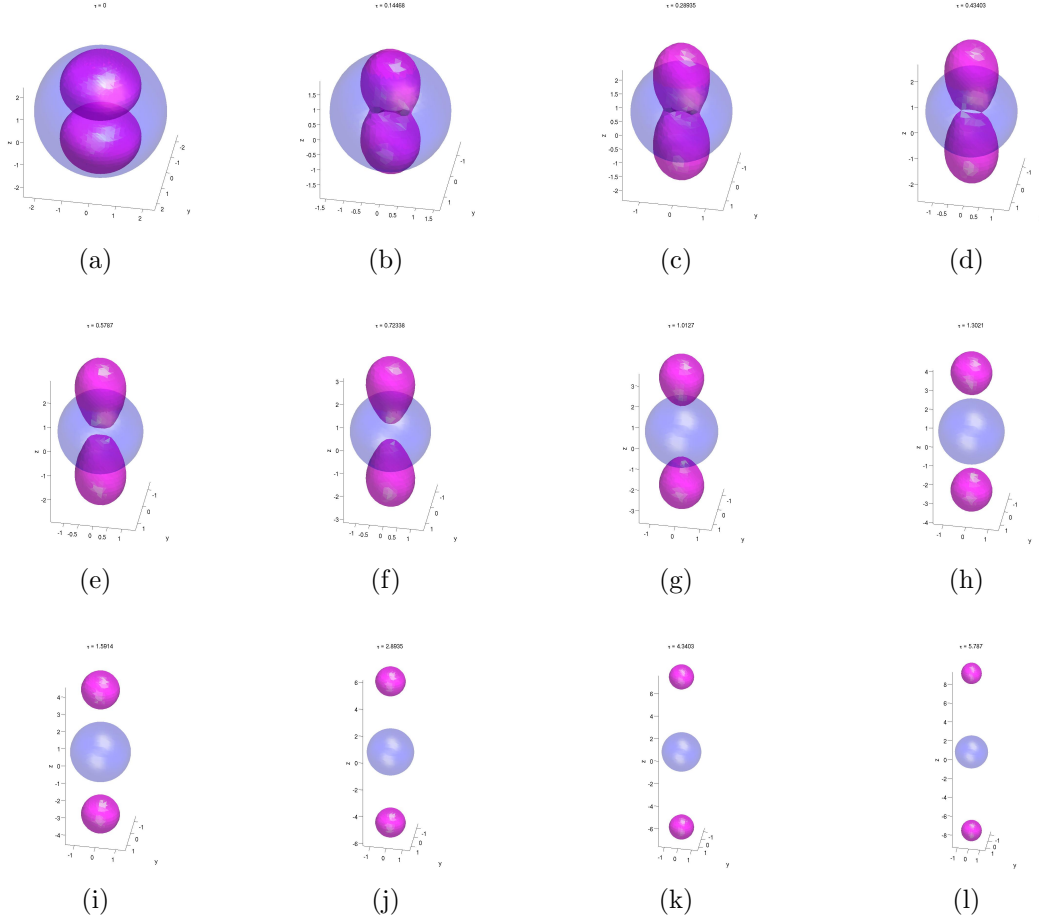


Figure 14: The global two-monopole of type B inside a single Skyrmion. The figures show isosurfaces of the monopole charge and Skyrmion charge densities, respectively, at half their respective maximum values. The blue surface is the Skyrmion charge and the magenta surface is the monopole charge. As the relaxation time progresses, the solution diverges and the monopoles eventually escape off to infinity. The calculation is made on a  $121^3$  cubic lattice.



to find a function  $\mathcal{G}$ , which multiplies the monopole Lagrangian, such that the monopole energy locally dominates over the Skyrmon energy. The problem of the, in this paper, chosen type of function, is that the constraint (5.8) needs to be satisfied. A different function that would not have such a constraint can be constructed as

$$\mathcal{G}(n_4) = \frac{1}{2} \left( \frac{1 + b - n_4^2}{2 + b} \right)^\alpha, \quad (6.1)$$

although this may be less stable than the function chosen in this paper because the energy barrier drops to the same value outside the Skyrmon as inside it. This type of function can be investigated in future works.

One potential application of these stable multimonomopole systems would be as potential models of dark matter halos [13, 14], as their density profiles asymptotically scale as  $1/r^2$ , automatically yielding flat rotation curves. The long distance divergences also need to be eliminated in this context, but various mechanisms for this have been proposed in the literature.

Finally, of course global multi-monopoles with charge  $Q > 2$  may equally well be considered in our construction. We leave this for future investigations.

## Acknowledgments

S. B. G. thanks Roberto Auzzi for discussions. J. E. is supported by NSFC grant 11375201. S. B. G. thanks the Recruitment Program of High-end Foreign Experts for support.

## Appendix A The unstable two-monopole

For completeness, we attempt to put the  $Q = 2$  monopole on a lattice with the initial condition given by the Ansätze (5.10) and (3.3) with  $d = h_x$ , i.e. the deformation parameter takes the values of a single lattice spacing. We take the profile function of the initial condition to be

$$h = \tanh[\kappa r],$$

where  $r$  is the radial coordinate and  $\kappa$  is an appropriately chosen constant. In Fig. 15 is shown a series of snapshots of the isosurfaces of the monopole charge as the relaxation time progresses. We observe that the two monopole constituents split up, escape the Skyrmon and move off to infinity (at an accelerating speed).

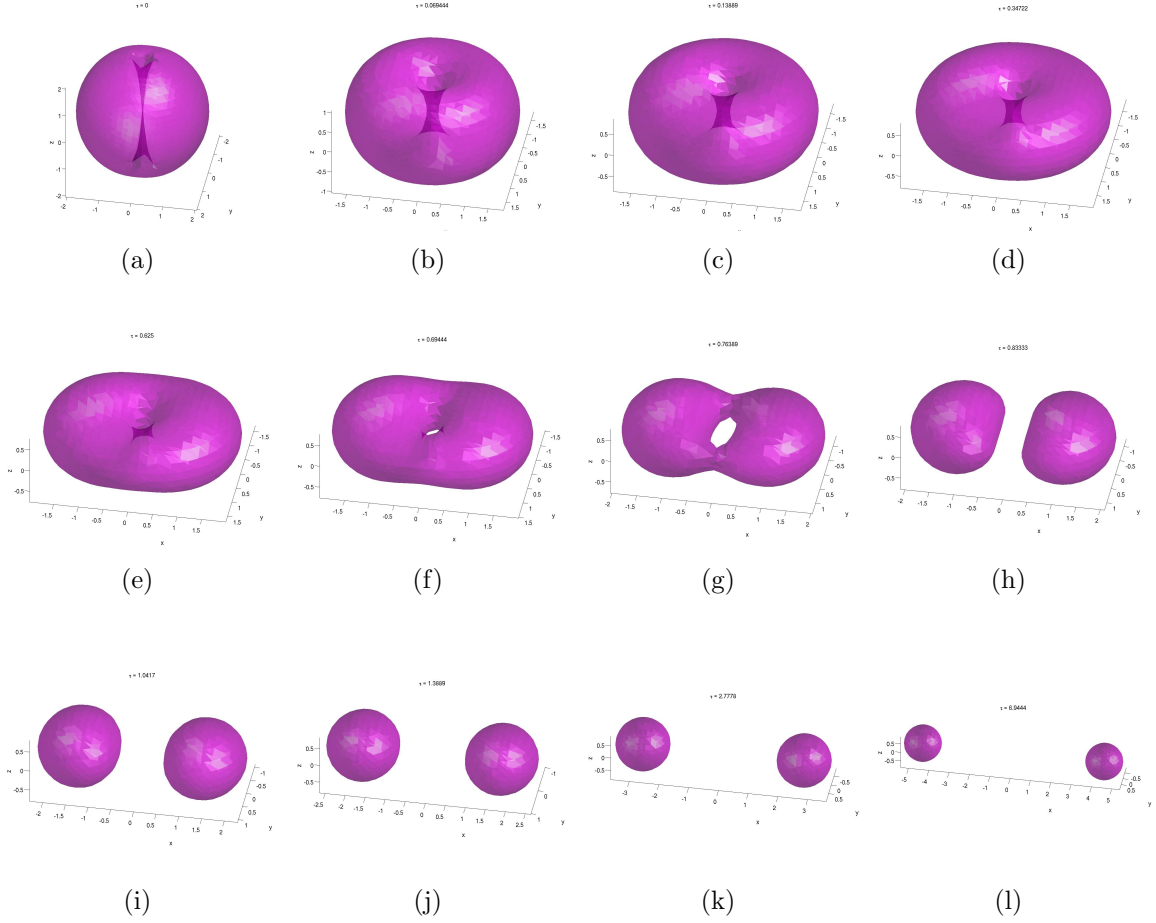


Figure 15: The global two-monopole of type A with deformation parameter  $d = h_x$ . The figures show isosurfaces of the monopole charge at half its maximum value. As the relaxation time progresses, the solution diverges and the monopoles eventually escape off to infinity. The parameters are chosen as  $v = 1/4$  and  $\lambda = 128$ . The calculation is made on a  $121^3$  cubic lattice.

## References

- [1] T. W. B. Kibble, “Topology of Cosmic Domains and Strings,” *J. Phys. A* **9**, 1387 (1976).
- [2] M. Barriola and A. Vilenkin, “Gravitational Field of a Global Monopole,” *Phys. Rev. Lett.* **63**, 341 (1989).
- [3] A. D. Linde, “Particle physics and inflationary cosmology,” *Contemp. Concepts Phys.* **5**, 1 (1990) [hep-th/0503203].
- [4] P. Poulin, D. A. Weitz, “Inverted and multiple nematic emulsions,” *Phys. Rev. E* **57**, 626 (1998).
- [5] A. S. Goldhaber, “Collapse of a ‘Global Monopole.’,” *Phys. Rev. Lett.* **63**, 2158 (1989).
- [6] S. H. Rhie and D. P. Bennett, “Global monopoles do not ‘collapse’,” *Phys. Rev. Lett.* **67**, 1173 (1991).
- [7] L. Perivolaropoulos, “Instabilities and interactions of global topological defects,” *Nucl. Phys. B* **375**, 665 (1992).
- [8] T. H. R. Skyrme, “A Unified Field Theory of Mesons and Baryons,” *Nucl. Phys.* **31**, 556 (1962);
- [9] T. H. R. Skyrme, “A Nonlinear field theory,” *Proc. Roy. Soc. Lond. A* **260**, 127 (1961).
- [10] Y. Brihaye, B. Kleihaus and D. H. Tchrakian, “Dyon - Skyrmion lumps,” *J. Math. Phys.* **40**, 1136 (1999) [hep-th/9805059].
- [11] S. B. Gudnason and M. Nitta, “Fractional Skyrmions and their molecules,” *Phys. Rev. D* **91**, no. 8, 085040 (2015) [arXiv:1502.06596 [hep-th]].
- [12] G. H. Derrick, “Comments on nonlinear wave equations as models for elementary particles,” *J. Math. Phys.* **5**, 1252 (1964).
- [13] J. Evslin and S. B. Gudnason, “Dwarf Galaxy Sized Monopoles as Dark Matter?,” arXiv:1202.0560 [astro-ph.CO].
- [14] J. Markar Evslin, “Giant monopoles as a dark matter candidate,” *J. Phys. Conf. Ser.* **496**, 012023 (2014) [arXiv:1311.1627 [astro-ph.CO]].